Copyright © 2007 American Scientific Publishers
All rights reserved
Printed in the United States of America

Journal of Nanoscience and Nanotechnology
Vol. 7, 2719–2725, 2007

Nanostructured GaN Nucleation Layer for Light-Emitting Diodes

J. Narayan[1,*] P. Pant[1], W. Wei[1], R. J. Narayan[2], and J. D. Budai[3]

[1] *Department of Materials Science and Engineering, EB-I, Centennial Campus, North Carolina State University, Raleigh, North Carolina 27695-7907, USA*
[2] *Department of Biomedical Engineering, UNC, Chapel Hill, North Carolina, USA*
[3] *Materials Science and Technology Division, Oak Ridge National Laboratory, Oak Ridge, Tennessee 37831-6030, USA*

This paper addresses the formation of nanostructured gallium nitride nucleation (NL) or initial layer (IL), which is necessary to obtain a smooth surface morphology and reduce defects in h-GaN layers for light-emitting diodes and lasers. From detailed X-ray and HR-TEM studies, researchers determined that this layer consists of nanostructured grains with average grain size of 25 nm, which are separated by small-angle grain boundaries (with misorientation ∼1°), known as subgrain boundaries. Thus NL is considered to be single-crystal layer with mosaicity of about 1°. These nc grains are mostly faulted cubic GaN (c-GaN) and a small fraction of unfaulted c-GaN. This unfaulted Zinc-blende c-GaN, which is considered a nonequilibrium phase, often appears as embedded or occluded within the faulted c-GaN. The NL layer contained in-plane tensile strain, presumably arising from defects due to island coalescence during Volmer-Weber growth. The 10L X-ray scans showed c-GaN fraction to be over 63% and the rest h-GaN. The NL layer grows epitaxially with the (0001) sapphire substrate by domain matching epitaxy, and this epitaxial relationship is remarkably maintained when c-GaN converts into h-GaN during high-temperature growth.

Delivered by Ingenta to:
Oak Ridge National Laboratory
IP : 160.91.46.82
Fri, 29 Jun 2007 13:27:23

Keywords: Gallium Nitride, Nanostructured Nucleation Layer, Light Emitting Diodes (LEDs), Domain Matching Epitaxy.

1. INTRODUCTION

Formation of high-quality gallium nitride and their alloys as thin films with reduced defect densities on sapphire substrates is the key to realization of high-efficiency light-emitting diodes and lasers.[1–6] MOCVD (metallorganic chemical vapor deposition) is now a well established technique for the growth of GaN and related alloys on sapphire substrates. The GaN growth on (0001) sapphire occurs primarily via three-dimensional (3D Volmer Weber) island growth.[6–8] In one step growth at high temperatures (≥1000 °C) these islands are relatively large and have h-GaN (Wurtzite) structure, but they result in a rough surface with a high-density of defects such as dislocations and pits, and, sometimes, grain boundaries with misorientations larger than 1–2°. Surface roughness and defects are undesirable for device fabrication. To obtain a less defective smooth surface, two-step growth has been proposed, where the first layer (about 25 nm thick) is grown at low temperatures (500–600 °C), known as LT layer and the second layer at higher temperatures (≥1000 °C), known as HT layer. The LT layer, also known as nucleation layer (NL) or initial layer (IL), which has cubic Zinc Blende (c-GaN) structure, provides a template for the HT layer having hexagonal Wurtzite (h-GaN) structure. Since structural defects such as dislocations and grain boundaries cannot end inside a crystal, the role of NL layer becomes very pivotal in our quest for achieving relatively "defect-free" device-quality h-GaN layer.[4–8]

In this paper, we characterize in detail the NL layer using atomic force microscopy (AFM), transmission electron microscopy (TEM), and X-ray diffraction (XRD) techniques.[9] Detailed X-ray θ, 2θ, and Φ scans show that NL layer (c-GaN structure) grows epitaxially with 30 or 90° in-plane rotation on (0001) sapphire substrate via domain matching epitaxy. The domain epitaxy is maintained upon transformation from c-GaN into h-GaN.[10] The NL layer (∼25 nm thick) consists of a unique nanocrystalline structure where grains are misoriented with respect to other by about a degree. These subgrains are faulted preferentially in one of the four {111} planes of c-GaN. We have determined relative fractions of c-GaN and h-GaN by using Hendricks-Teller model[11] to calculate X-ray diffraction intensities and match with experimental results.

*Author to whom correspondence should be addressed.

2. EXPERIMENTAL DETAILS

The GaN nucleation layers were grown on (0001) sapphire substrates using MOCVD growth technique[6] grown by Kopin Corporation. The (0001) sapphire substrates were cleaned with solvents and treated with flowing H_2 and NH_3 at 1100 °C. The nucleation (low-temperature, LT) layers were grown in the temperature range of 500–600 °C with a nominal thickness ranging from 7 to 40 nm. This is characterized as the first-step growth. During MOCVD growth, trimethylgallium (TMGa) and ammonia (NH_3) were used as precursors for Ga and N, respectively. Microstructural and growth characteristics of these initial layers were investigated using conventional and high-resolution TEM (transmission electron microscopy), X-ray diffraction (θ, 2θ, and Φ scans using CuKα radiation with $\lambda = 0.154$ nm) and AFM (atomic force microscopy) techniques. HRTEM in cross-section was used to study thin film growth characteristics after first and second-step growth processes. The second step and subsequent growth of GaN was carried out in the temperature range ≥1000 °C to produce device quality GaN layers.

Delivered by Inger
Oak Ridge National L
IP : 160.91.48.
Fri, 29 Jun 2007 13

3. RESULTS AND DISCUSSION

Figures 1(a) and 1(b) show AFM micrographs from 7 nm thick and 40 nm thick NL layers, respectively, grown at 530 °C. The GaN grows by three-dimensional island growth (Volmer-Weber Growth), where the islands form a contiguous beady structure. The average size of the islands is about 25 nm, which become subgrains in nanocrystalline thin films. Since these subgrains are separated by subgrain boundaries with average misorientation of 1°, the NL is considered essentially a single-crystal layer with mosaicity of about 1°.

Figure 2 shows low-resolution θ–2θ scans along the Al_2O_3[0001] substrate direction plotted with a logarithmic scale for 40 nm thick GaN NL layer. This scan contains the intense Al_2O_3(0006) peak along with the less intense c-GaN(111) and c-GaN(222) peaks. However, for a θ–2θ scans along this direction, c-GaN(111) and c-GaN(222) peaks overlap with h-GaN(0002) and h-GaN(0004) peaks, respectively. Therefore, from this scan alone, it is not possible to distinguish between c-GaN and h-GaN phases of the film. On the other hand, the L-scans to be discussed below provide information on the relative fraction of c-GaN and h-GaN phases.[9]

Figure 3(a) shows a high-resolution θ–2θ scan through the cubic Ga(111) peak taken using a Ge(111) –crystal analyzer. The $\Delta 2\theta$ FWHM (full-width-at-half maximum) of 0.19 degrees indicates the c-GaN film to be of high crystalline quality. Using the Scherrer equation, we can estimate the thickness (t) of the c-GaN film scattering coherently. The thickness (t) is given by $t = 0.9\lambda/(B \cos \theta_B)$, where λ is X-ray wavelength, 0.154 nm; B is the FWHM in radians, and θ_B is the Bragg angle. From this,

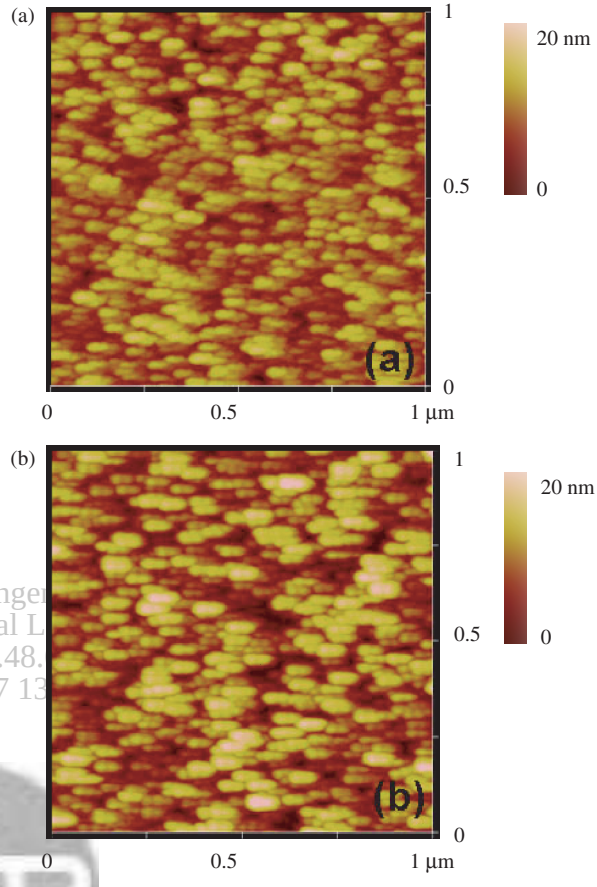

Fig. 1. AFM micrographs from NL layers showing three-dimensional (island) structure: (a) 7 nm thick NL layer; (b) 40 nm thick NL layer.

the thickness is calculated to be ∼42 nm, in agreement with cross-section TEM data. Figure 3(b) shows θ-scans (rocking curves) through the cubic GaN (111) peak at different Φ (0°, 180°, 90°, −90°) positions. The superposition of the scans show that the GaN(111) planes are well aligned on average parallel to the Al_2O_3(0001) planes. The $\Delta\theta$ (FWHM) is ∼1.3°, showing the mosaicity of the film or the average misorientation between the subgrains in the film by this amount. It is interesting to note that the rocking curve exhibits a triangular shape, which may be related

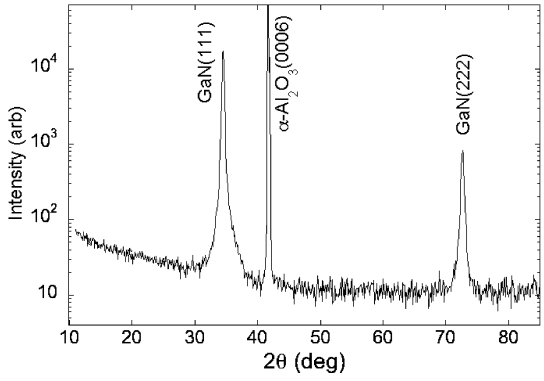

Fig. 2. X-ray low-resolution θ–2θ scans along the Al_2O_3 [0001] substrate with a logarithmic scale.

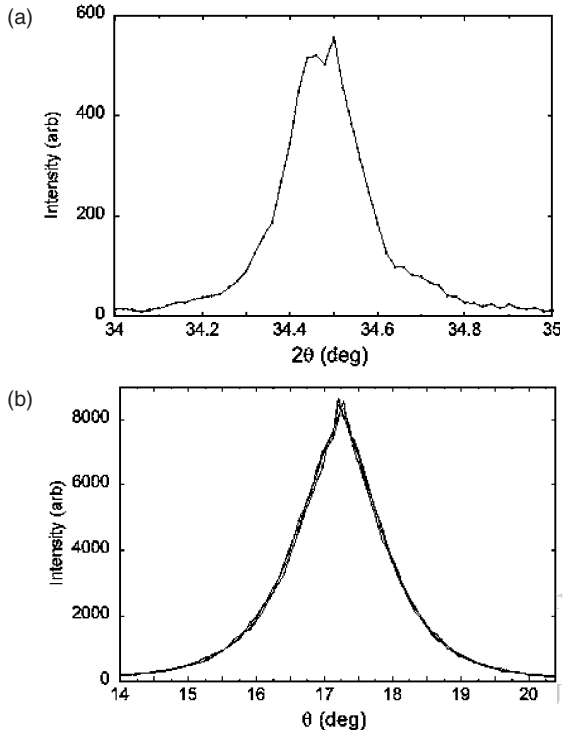

Fig. 3. (a) X-ray high-resolution θ–2θ scan through the cubic Ga (111) peak, showing the FWHM (full-width-at-half maximum) of 0.19 degrees; and (b) θ-scans (rocking curves through the cubic GaN (111) peak at different Φ (0, 180, 90, −90) degree positions.

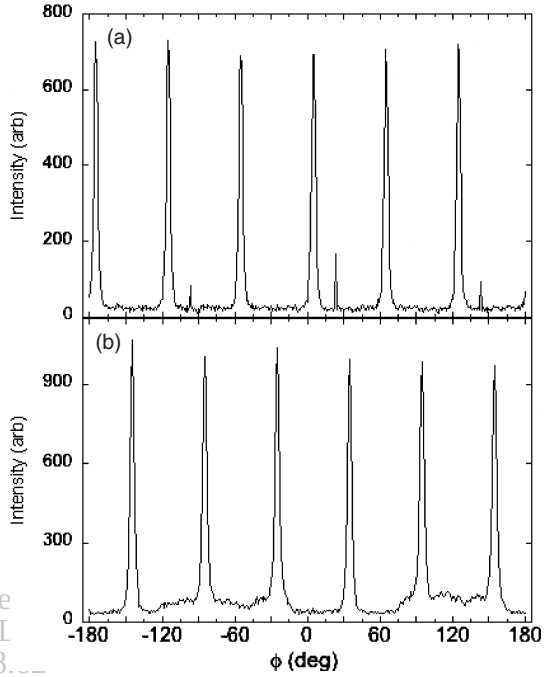

Fig. 4. (a) X-ray Φ scan at hexagonal h-GaN(112) or c-GaN(3–11), showing film as well as substrate peaks and their relative orientation; (b) Φ scan at GaN (1 0 3/4) in hexagonal coordinates with well-defined six c-GaN peaks again verify high-quality epitaxy of the film.

to a unique distribution of strains associated with stacking faults in different subgrains of the film.[12–13]

Figure 4(a) is a Φ scan through c-GaN{3–11} peaks, which have an equivalent d-sacing as h-GaN{112}, where six c-GaN peaks along with three Al_2O_3 substrate peaks are clearly shown. This result verifies the epitaxial nature of the c-GaN film as well as the expected in-plane 30° rotation (using h-GaN indexation) with respect to the Al_2O_3 substrate. Using c-GaN indexation, ⟨1–10⟩ c-GaN aligns with ⟨10–10⟩ of Al_2O_3. Figure 4(b) shows another Φ scan near the c-GaN{1–11}, where six well-defined c-GaN peaks again verify high-quality epitaxy of the film. From the high-resolution X-ray scans, we determined that c-GaN is slightly slightly distorted with $a = b = 0.4513$ nm, and $\alpha = \beta = \gamma = 90.12°$. For an equivalent h-GaN phase, we found $a = b = 0.3195$ nm, $c = 0.5199$ nm; and $\alpha = \beta = 90°$, and $\gamma = 120°$. This result implies the presence of in-plane tensile strain. In contrast, previous studies of high-temperature h-GaN growth on sapphire (0001) substrates reported compressive strain due to differences in coefficients of thermal expansion (h-GaN $= 5.59 \times 10^{-6}$/K in a-direction; Sapphire $= 7.5 \times 10^{-6}$/K in a-direction).[14] In the present low temperature growth, the tensile strain due to c-GaN island coalescence during Volmer-Weber growth appears to dominate.[15–16]

Now we turn to L-scans (10 L scans in hexagonal coordinates) which provide information on relative fraction of c-GaN and h-GaN.[9] It should be noted that a stacking fault in c-GaN locally transforms the region into h-GaN, and by inserting stacking faults in alternate {111} planes, we can transform the region completely from c-GaN (ABCABCABCABC stacking) into h-GaN (ABABABABAB stacking). Since c-GaN is a nonequilibrium phase with a higher Gibbs free energy, it is surmised that the system (film) tends to reduce its energy by introducing stacking faults and transform into the equilibrium h-GaN phase of lower free energy. The 10 L scan shows broad peaks which are not located either at integral positions (corresponding to pure h-GaN phase) or at L/3 ($L = 0.67, 1.33, 2.67, 3.33..$), corresponding to pure c-GaN phase. From the Hendricks-Teller (H-T) model, we are able to obtain a good agreement for 63% c-GaN and 37% h-GaN, as shown in Figure 5. The (10 L) X-ray scans exhibit an intensity peak at $L = 2.66$, which corresponds to pure c-GaN, indicating the presence of unfaulted c-GaN in agreement with TEM data. The Hendricks-Teller model was applied to analyze relative fraction c-GaN and faulted c-GaN (h-GaN) in the NL layer grown 530 °C. In this model, X-ray diffraction pattern was calculated by taking into account the scattering power of each of the layers. Since these atomic layers could form either hexagonal or cubic phase by different stacking sequence, a statistical correlation was considered in the modeling calculation. By listing out all the possible stacking sequences, the probability of either hexagonal or cubic phase was incorporated into the model. By using Eq. (34) in Ref. [11] of H-T model, we calculated diffraction intensity as a function of L, which was corrected for Lorenz-polarization factor, geometrical correction factor

red by Inge
National I
160.91.48.
Jun 2007 13:27:23

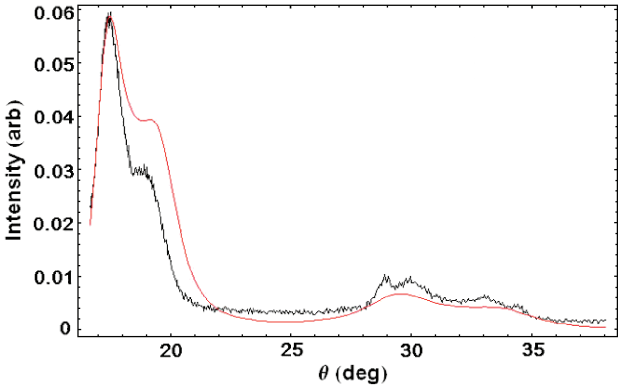

Fig. 5. X-ray low-resolution L-scan (10 L scans in hexagonal coordinates) and H-T model calculation for 64% c-GaN and 36% h-GaN.

and atomic scateering factors of Ga and N.[17] The calculated intensity was fitted to the experimental X-ray data to estimate the density tacking faults (or the fraction of h-GaN phase) in the NL layer. It was found fraction of hexagonal phase is 0.63, which fits the experimental data quite well, as shown in Figure 5. Thus the fraction of hexagonal phase was estimated to be 0.37, roughly one stacking fault in every three layers.

Now we present the details of complementary TEM studies using cross-section samples. Figure 6(a) shows a TEM cross-section where the GaN film is about 40 nm thick with a sharp film-substrate interface. The selected-area-diffraction pattern (Fig. 6(b)), covering both the film and the substrate regions, shows an epitaxial relationship of c-GaN with the sapphire. The streaking in the pattern is due to stacking faults in {111} c-GaN which become basal {0001} planes of h-GaN. The stacking faults in alternate layers of c-GaN phase lead to formation of h-GaN phase. These parallel (111) c-GaN and (0001) h-GaN layers produce streaking and secondary diffraction spots along ⟨111⟩ or ⟨0001⟩ directions, as observed in Figure 6(b). The streaking along the ⟨111⟩ direction of Zinc Blende GaN results from the presence of high density of individual stacking faults, where the length of the streak is inversely proportional to the thickness of the fault. While the stacking faults create hexagonal regions locally, they are not present in the alternate layers to produce a large region of hexagonal GaN phase. There is some evidence of twinning, as indicated by the intensity along the one-third ⟨111⟩ directions in the ⟨110⟩ SAD diffraction pattern. In addition, the secondary diffraction spots result from a regular stacking of the faults. The c-GaN film grows epitaxially on (0001) sapphire substrate via domain matching epitaxy, where integral multiples of planes match across the film-substrate interface (10). The c-GaN has the following epitaxial relationship: $\langle 111\rangle_{c-GaN}$// $\langle 0001\rangle_{sap}$, $\langle 110\rangle_{c-GaN}$// $\langle 10\text{–}10\rangle_{sap}$, and $\langle 211\rangle_{c-GaN}$// $\langle -2110\rangle_{sap}$. In terms of planar matching, (220) planes of c-GaN match with (30–30) planes of sapphire, and 1/3(422) planes of c-GaN match with (−2110) planes of sapphire in the perpendicular direction. The transformation from c-GaN into h-GaN involves the transformation of (220) planes of c-GaN into (−2110) planes of h-GaN and 1/3(422) planes of c-GaN into (30–30) planes of h-GaN, and the epitaxial relationship changes to: $\langle 0001\rangle_{h-GaN}$// $\langle 0001\rangle_{sap}$ and $\langle -2110\rangle_{h-GaN}$// $\langle 10\text{–}10\rangle_{sap}$. In terms of planar matching epitaxy, (−2110) planes of h-GaN match with (30–30) planes of sapphire, and, in the perpendicular direction, (30–30) planes of h-GaN match with (−2110) planes of sapphire. This epitaxial relationship is known as 30° or 90° rotation. It is interesting to note that relative spacing for c-GaN as well as h-GaN planes remains the same during this transformation because of a(c-GaN) = $\sqrt{2}$ a(h-GaN) = $\sqrt{3}$ c(h-GaN)/2 equivalence between lattice constants of cubic and hexagonal structures. The transformation from cubic to hexagonal structure can occur via insertion or removal of stacking faults in {111} planes of c-GaN and {0001} planes of h-GaN. The hexagonal structure is preferred as a template for higher-temperature growth, however, the cubic structure having defective hexagonal phase with stacking faults in alternate layers, can also provide a template for epitaxy. The Shockley partials associated with stacking faults, which appear at the island edges, provide sources for undesirable threading dislocations[6].

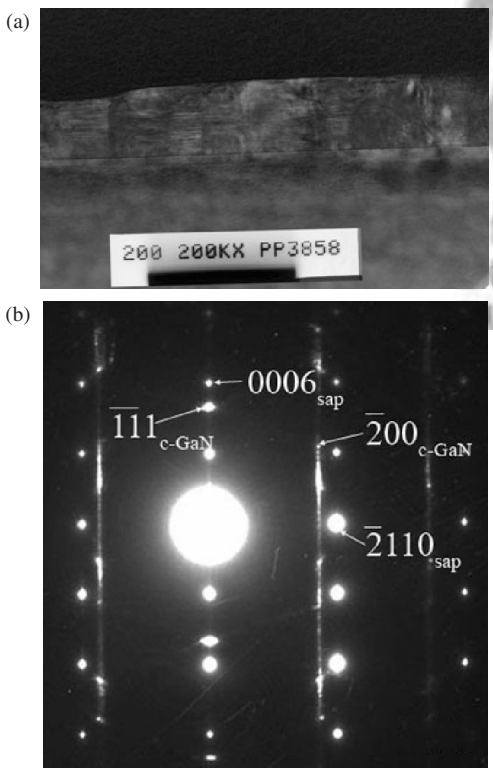

Fig. 6. (a) Cross-section (low-resolution) TEM micrograph from 40 nm thick film; (b) corresponding selected-area-diffraction pattern showing c-GaN and sapphire diffraction spots. The streaking shows the presence of thin stacking faults and multiple diffraction spots indicate a regularly stacked fault structure, in addition to twins.

High-resolution cross-section TEM was done to obtain the details of defects and interfaces in the NL layer.

Delivered by Ingenta to:
Oak Ridge National Laboratory
IP: 160.91.48.62
Fri, 30 Jun 2007 13:27:23

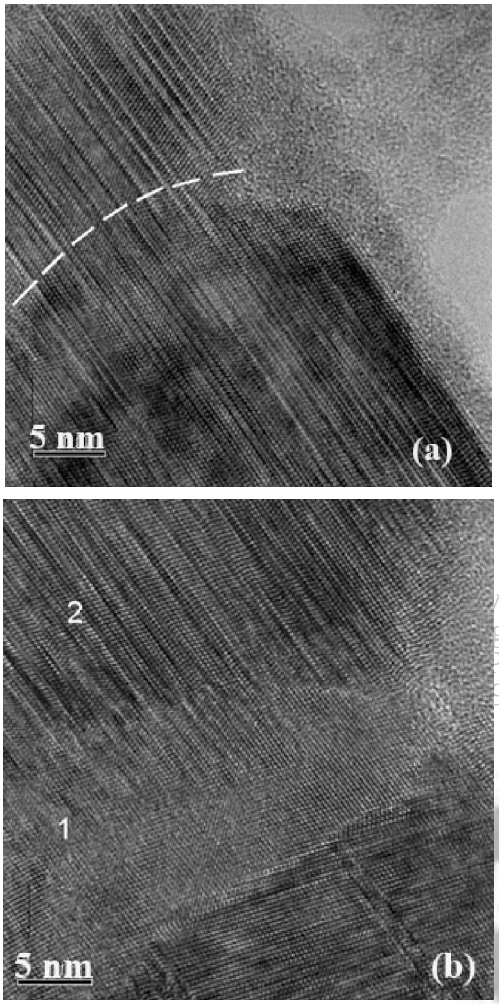

Fig. 7. (a) High-resolution cross-section TEM micrograph from 40 nm thick film where the dotted line shows the boundary of two subgrains faulted in the same {111} planes; (b) Unfaulted c-GaN subgrain (#1) is surrounded by c-GaN subgrains (#2 and 3) faulted in different {111} planes.

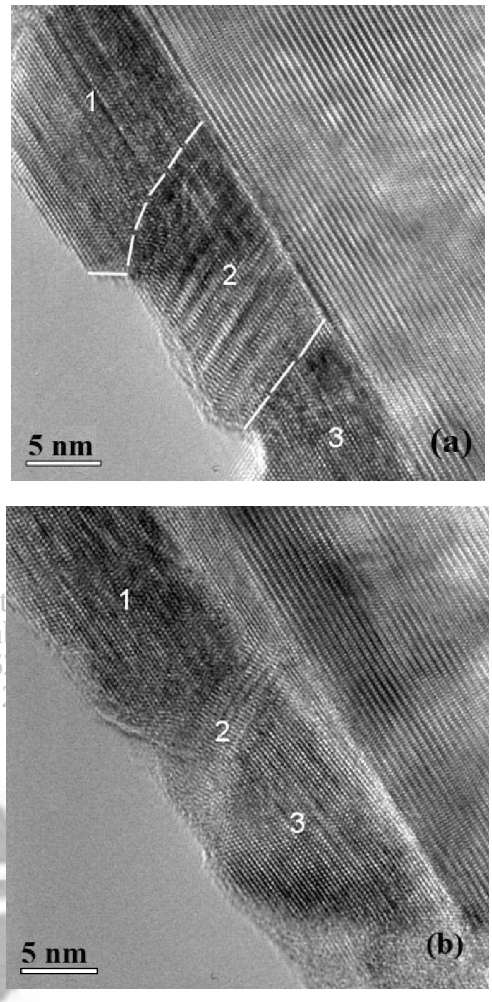

Fig. 8. (a) High-resolution cross-section TEM micrograph from 7 nm thick film where the dotted lines show the boundary of two subgrains faulted in different {111} planes; (b) c-GaN subgrains (#1 and #3) are connected by a twinned subgrain (#2).

vered by Ingent
ge National La
P : 160.91.48.6
9 Jun 2007 13:
ASP
AMERICAN SCIENTIFIC PUBLISHERS

Figure 7(a) shows two subgrains in c-GaN, which are heavily faulted in the same {111} planes that are parallel to the (0001) sapphire substrate. The interface boundary is indicated by dotted lines and the angle is estimated to be less than 1°. In Figure 7(b), there is unfaulted c-GaN subgrain (labeled #1) which is enclosed by faulted c-GaN subgrains (2 & 3). It is interesting to note that faulting in grain 2 has occurred in the {111} planes different from that in subgrain #3. The unfaulted c-GaN grains tend to be enclosed or occluded by faulted c-GaN subgrains, which have higher growth velocities. The c-GaN is a nonequilibrium phase with a higher Gibbs free energy, however, it can lower its energy by introducing stacking faults which have h-GaN phase locally. The mechanism of conversion of c-GaN into h-GaN by stacking faults has been discussed in detail previously.[6]

To investigate the initial stages of growth characteristics of NL layer, we have investigated the details of microstructures in a film grown for a fraction of the time needed to grow a full NL layer. Figure 8(a) shows high-resolution TEM cross-section micrographs from NL layer with average thickness about 7 nm. The HRTEM micrograph shows three subgrains with 25 nm width and 7–10 nm height. It is interesting to note that all the grains have grown epitaxially, but subgrain 2 is faulted in different {111} plane at an angle from the film-substrate interface, whereas subgrains 1 & 3 are faulted in {111} planes parallel to the interface. Figure 8(b) shows three epitaxial subgrains, where subgrains 1 & 3 are faulted in {111} planes parallel to the interface, but subgrain 2 in the middle is related to the other subgrain through a twin. Thus, all the subgrains in the NL layer have the same epitaxial relationship with (0001) sapphire substrate, but they are faulted predominantly along one of the four {111} planes of c-GaN.

In the following, we analyze the characteristics of c-GaN and h-GaN epitaxy over the (0001) sapphire substrate. The high-resolution cross-section TEM (in Fig. 9(a)) and

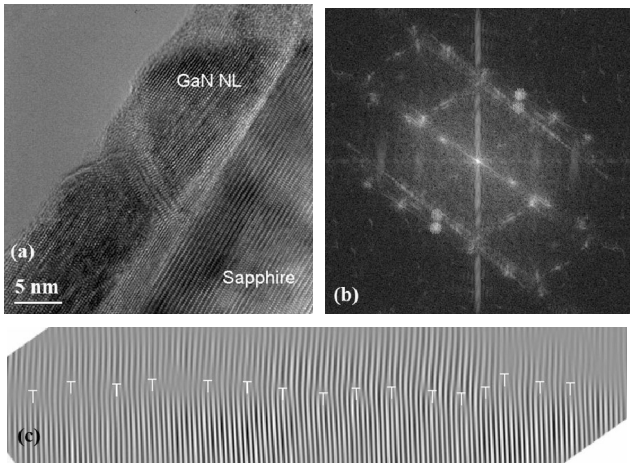

Fig. 9. (a) High-resolution TEM cross-section image of c-GaN; (b) corresponding FFT diffraction pattern; and (c) FFT image of the interface demonstrating matching of integral multiples of lattice planes (domain matching epitaxy) across the c-GaN/sapphire interface. There is one dislocation contained in each domain.

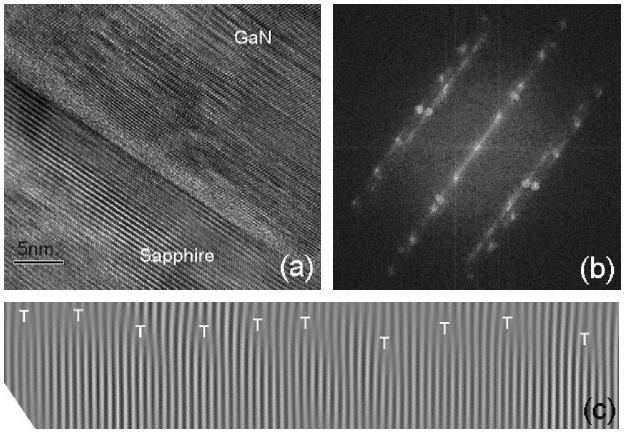

Fig. 10. (a) High-resolution TEM cross-section image of c-GaN; (b) corresponding FFT diffraction pattern; and (c) FFT image of the interface demonstrating matching of integral multiples of lattice planes (domain matching epitaxy) across the h-GaN/sapphire interface. There is one dislocation contained in each domain.

Delivered by Ingenta to:
Oak Ridge National Laboratory
IP: 160.91.46.92
Fri, 29 Jun 2007 15:22:23

corresponding FFT diffraction patterns (in Fig. 9(b)) clearly demonstrate the epitaxial growth of c-GaN on the (0001) substrate. The inset FFT diffraction patterns from the film-substrtae shows ⟨110⟩ c-GaN // ⟨10–10⟩ diffraction patterns. In the cross-section along the interface 1/3(422) planes (with planar spacing of $\sqrt{3}\ a_c/2\sqrt{2}$) are aligned with (−2110) planes of sapphire. The matching of these planes is shown in the FFT image, where there is a missing plane (dislocation) within each domain (Fig. 9(c)). This epitaxy of GaN occurs via domain matching epitaxy, where integral multiples of lattice planes match across the GaN/α-Al2O3 interface. Upon annealing or direct high-temperature growth, the nucleation layer transforms into h-GaN, where 1/3(422) c-GaN spot turns into (10–10) spot of h-GaN (with planar spacing of $\sqrt{3}\ a_h/2$). The transformation follows the equivalence of a(c-GaN) = $\sqrt{2}$ a(h-GaN) = $\sqrt{3}$ c(h-GaN)/2 between cubic (face-centered) and hexagonal (close packed) structures. This h-GaN matching on sapphire is shown in high-resolution cross-section image (Fig. 10(a)) with corresponding FFT diffraction pattern (Fig. 10(b)) and FFT image (Fig. 10(c)). The figure shows alternating 6/7 and 7/8 film/substrate planes matching across the interface, which is in agreement with new paradigm of domain matching epitaxy for the formation of single-crystal films on substrates with large lattice misfits.[6,10] According to the DME paradigm, for a complete relaxation of misfit strain, three 6/7 domains should alternate with one 7/8 domain for GaN growth at 530 °C.[6,10]

In summary, the nucleation layer, when grown by MOCVD in the temperature range 500–600 °C, consists of predominantly faulted c-GaN and a small fraction of unfaulted c-GaN. The NL grows epitaxially on the (0001) sapphire substrate with a 30° or a 90° rotation via domain matching epitaxy. The c-GaN epitaxy is maintained when c-GaN converts into h-GaN during subsequent high-temperature growth. The NL has a unique nanostructure as it consists of nanocrystalline subgrains which are misoriented with respect to each other by an average angle of 1.3°. Each subgrain is faulted predominantly in one of the four {111} planes of c-GaN. If this initial misorientation increases beyond a critical point (somewhere 2–3° range) then the quality of subsequent h-GaN grown at higher temperatures decreases as the high density of dislocations from these boundaries continue into the active region of the device. It is surmised that this happens if h-GaN is grown at ≥1000 °C on (0001) sapphire substrate directly in a single step. This explains why single-step h-GaN growth at high temperatures results in a rough surface (corresponding to larger subgrains) and high-density of propagating threading dislocations.

Acknowledgments: This research was partly supported by the National Science Foundation and Kopin Corporation. The work also supported by the DOE Office of Science, DMS under contract with ORNL, managed by UT-Battelle, LLC. We thank Carol Thompson, and G. Brian Stephenson and Jon Tischler for very helpful discussions.

References and Notes

1. S. Strite and H. Morkoc, *J. Vac Sci. Technol. B* 10,1237 (**1992**).
2. S. J. Pearton, J. C. Zolper, R. J. Shul, and F. Ren, *J. Appl. Phys.* 86, 1 (**1999**).
3. S. C. Jain, M. Willander, J. Narayan, and R. V. Overstraeten, *J. Appl. Phys.* 87, 965 (**2000**).
4. X. H Wu, L. M. Brown, D. Kapolnek, S. Keller, S. P. DenBaars, and J. S. Speck, *J. Appl. Phys.* 80, 3228 (**1996**).
5. X. H. Wu, D. Kapolnek, E. J. Tarsa, B. Heying, S. Keller, B. P. Keller, U. K. Mishra, S. P. DenBaars, and J. S. Speck, *Appl. Phys. Lett.* 68, 1371 (**1996**).
6. J. Narayan, P. Pant, A.Chugh, H. Choi, and J. C. C. Fan, *J. Appl. Phys.* 99, 054313 (**2006**).
7. K. Lorenz, M. Gonsalves, W. Kim, V. Narayanan, and S. Mahajan, *Appl. Phys. Lett.* 77, 3391 (**2000**).

8. V. Narayanan, K. Lorenz, W. Kim, and S. Mahajan, *Phil Mag A* 82, 885 (**2002**).
9. A. Munkohlm, C. Thomson, C. M. Foster, J. A. Eastman, O. Auciello, G. B. Stephenson, P. Fini, S. P. DenBaars, and J. S. Speck, *Appl. Phy. Lett.* 72, 2972 (**1998**).
10. J. Narayan and B. C Larson, *J. Appl. Phys.* 93, 945 (**2003**).
11. S. Hendricks and E. Teller, *J. Chem. Phys.* 10, 147 (**1942**).
12. J. G. E. Klappe and P. F. Fewster, *J. Appl. Crst.* 27, 103 (**1997**).
13. Z. Zhang, C. C. Kao, D. P. Siddous, and J. B. Hastings, *Acta Cryst. A* 58, 487 (**2002**).
14. T. Detchprohm, K. Hiramatsu, K. Itoh, and I. Akasaki, *Jpn. J. Appl. Phys.* 31, L1454 (**1992**).
15. S. C. Seel, J. J. Hoyt, E. B. Webb, and J. Zimmerman, *Phy Rev B* 73, 245402 (**2006**).
16. W. D. Nix and B. M. Clemens, *J. Mat. Res.* 14, 3467 (**1999**).
17. B. D. Cullity, Elements of X-Ray Diffraction, Addison-Wesley Publishing Company (**1966**), Chap. 4.

Received: 10 November 2006. Accepted: 21 January 2007.

Delivered by Ingenta to:
Oak Ridge National Laboratory
IP : 160.91.48.62
Fri, 29 Jun 2007 13:27:23

AMERICAN SCIENTIFIC PUBLISHERS